Chemometric methods applied to FTIR spectra to discriminate treated and non-treated cutaneous malignant lesions from healthy skin

Cassio Lima, Viviane Goulart, Denise Zezell
Instituto de Pesquisas Energeticas e Nucleares, Universidade de São Paulo, São Paulo, 05508-000, Brazil
zezell@usp.br

Abstract: Chemometric methods were used to differentiate FTIR spectra of treated and non-treated malignant lesions from healthy skin. We conclude that the method can be used to evaluate the biological changes promoted by photodynamic treatment.
OCIS codes: (170.4580) Medical optics and biotechnology – Optical diagnostics for medicine; (170.6510) Medical optics and biotechnology – Spectroscopy, tissue diagnostics; (170.1580) Medical optics and biotechnology – Chemometrics.

1. Introduction

In recent years, the Fourier Transform Infrared Spectroscopy (FTIR) has successfully characterized the biological tissues. Due to its molecular-level information, the FTIR technique has great potential to differentiate neoplastic from normal cells, making it a possible and powerful diagnostic tool [7].

The use of vibrational spectroscopic methods associated to multivariate statistical techniques have been succeeded in discriminating skin lesions from normal tissues [1-4]. However, there are few studies exploring the potential of these techniques to assess the alterations promoted by photodynamic effect in tissue [5]. In this way, the present study aims to demonstrate the ability of ATR-FTIR spectroscopy associated to hierarchical cluster analysis (HCA) to evaluate the biochemical changes caused by photodynamic therapy (PDT) in skin neoplastic tissue.

2. Material and Methods

Chemical carcinogenesis and sample preparation

Neoplastic lesions were induced on Swiss mice using a well-established multi-stage chemical-carcinogenesis protocol [6]. At the end of chemical carcinogenesis, the animals were divided into four groups: healthy skin (G1), non-treated neoplastic tissue, neoplastic tissue submitted to PDT using ALA (G2) and MAL (G3). Animals from G3 group were submitted to a single-session of PDT using a photosensitizer cream prepared with active principle being ALA (20%) with other ingredients kept confidential (patent pending PIN°0705591-9). The same formulation was also used for the PDT performed in the animals from G4 group, only replacing the 5-aminolevulinic acid by its methyl ester MAL (10%). The cream was applied on the tumor lesions with 5-mm additional margin using a disposable plastic spatula and the excess was removed with a gauze before PDT. Light irradiation was performed using a prototype of LEDs emitting at 630 nm with fluence-rate of 5 mW/cm^2 and fluence of 12 J/cm^2. Biological tissues obtained with excisional biopsies were formalin-fixed and paraffin-embedded (FFPE). Sample sections with 5 µm thickness were obtained and placed in MirrIR low-E-coated slides (Kevley Technologies, Chesterland, OH, USA) and submitted to dewaxing protocol before for spectroscopic analysis.

FT-IR Spectroscopy

Spectra were collected using a Fourier transform infrared spectrometer (Thermo Nicolet 6700, Waltham, MA, USA) operating with an Attenuated Total Reflectance (ATR) accessory as sampling mode (Smart Orbit, Thermo Scientific, Waltham, MA, USA). Measurements were performed in medium infrared region (4000-400 cm^{-1}) with spectral resolution of 4 cm^{-1} and 100 scans per spectrum. Samples were pressed into ATR diamond crystal with standardized pressure and each spectrum obtained represents the averaged from 10 replicates measured in each sample. ATR-FTIR spectra were vector-normalized and second derivative of absorbance was calculated to reduce baseline offset and assess the overlapping sub-bands in row spectrum. For signal-smoothing, spectra were submitted to Savitzky–Golay filter with a polynomial of second order in an eleven points window.

3. Results and Discussion

Figure 1 shows the fingerprint region (900-1800 cm^{-1}) of averaged ATR-FTIR spectra and their second derivatives. The vibrational modes depicted in the Figure 1 have been frequently used in the spectroscopic studies of biological tissues and are associated to important cell content.

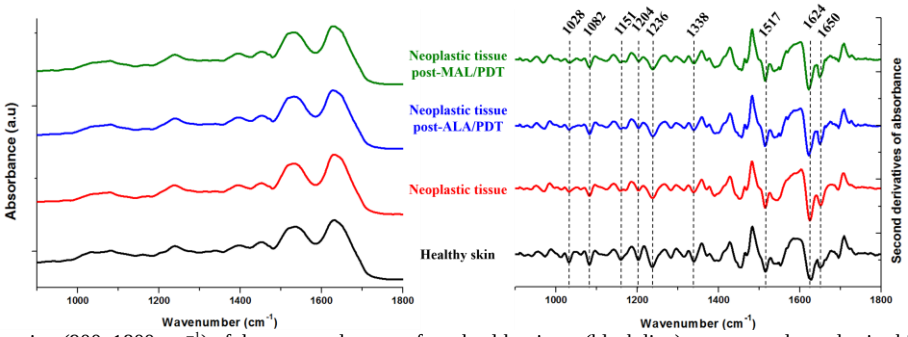

Fig. 1. Fingerprint region (900–1800 cm^{-1}) of the averaged spectra from healthy tissue (black line), non-treated neoplastic skin (red), neoplastic tissue post-ALA/PDT (blue) and neoplastic tissue submitted to MAL-PDT of normal (red line). Normalized spectra are shown in the left and the second derivatives in the right.

Similar vibrational modes were observed in all groups, with subtle differences in the absorption intensities. Spectral range from 1500-1700 cm^{-1} provide information about the protein content. Band at 1517 cm^{-1} relates to the Amide II and the sub-bands peaking at 1650 and 1624 cm^{-1} (Amide I region) are associated to the α-helix and β-sheet secondary structure of proteins. The vibrational modes at 1338, 1236 and 1204 cm^{-1} are associated to the collagen fibers and the bands peaking at 1028, 1082 and 1151 cm^{-1} are related to C-O and C-C stretching and C-O-H deformation motions from glycogen molecules [7]. Considering that the tissue-sample analysis is much more complex than the simple explanation of the features of single component vibration and that the effect of each structure may interact with the others and result in the amplification or reduction of a specific signature, we performed a pairwise comparison of each neoplastic group (treated and non-treated) against healthy skin. For this, the data were submitted to HCA aiming to calculate the accuracy of discrimination (AD) in each pairwise comparison. Figure 2 shows the dendrogram obtained with HCA using spectra from healthy and neoplastic skin as input.

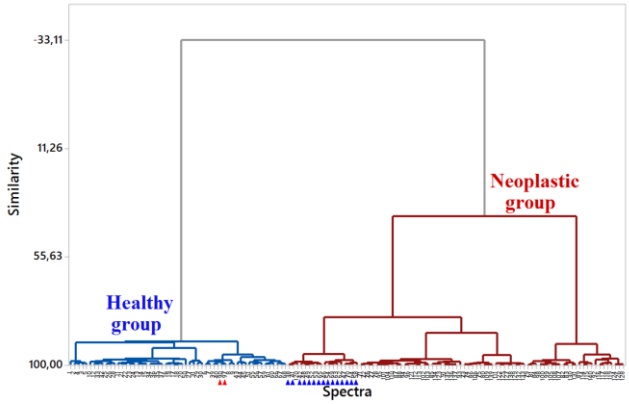

Fig. 2. Classification of the dataset into two categories (Healthy group in blue and neoplastic in red). The triangles in blue depict false positives and red triangles represent false negatives.

Samples listed 1-70 correspond to the spectra collected from healthy skin, whereas those listed as 70-140 represent the spectra obtained for neoplastic tissue. The distribution of all spectra used as input is shown in the abscissa axis and the distance of spectra within the same cluster is depicted in the ordinate axis. For the calculus of the AD in each pairwise comparison, we considered the true positive as the neoplastic spectra in the neoplastic group; true negative as the healthy skin spectra in the healthy group; the false positive as healthy spectra in the neoplastic group; and false negative as neoplastic spectra in the healthy group. The triangles in blue depict false positives and red triangles represent the false negatives. For the other pairwise comparison (Healthy *versus* Neoplastic post-ALA/PDT and Healthy *versus* Neoplastic post-MAL/PDT) we used the same argument, only replacing the non-treated neoplastic data for the spectra collected from neoplastic skin submitted to PDT. The AD values obtained with the pairwise comparison of healthy skin against the other groups are showed in the Figure 3.

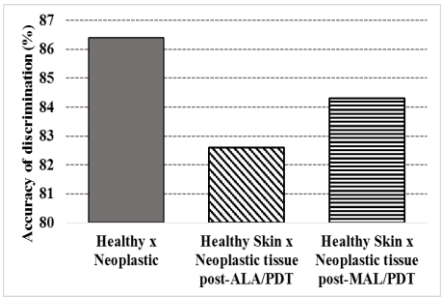

Fig. 3. Accuracy of discrimination obtained with clustering classification.

The value obtained for the accuracy of discrimination of HCA applied to FTIR spectra is an indirect parameter to assess the similarity of spectral dataset used as input, once that the ability of classification obtained with HCA depends on similarity level between the data analyzed. So that, higher values for the accuracy of discrimination indicate greater difference between the analyzed data. Thus, considering that the AC value obtained with the pairwise comparison of Healthy *versus* Neoplastic skin was the highest one, we can conclude that this group present biochemical features with lower similarity against the healthy tissue. Furthermore, the neoplastic tissue submitted to PDT with both photosensitizers presented biochemical characteristics more similar to those of normal tissue, which may be used as an indicative of the treatment.

4. Conclusions

HCA obtained satisfactory accuracy to discriminate ATR-FTIR spectra of non-treated and post-PDT neoplastic lesions from healthy skin. Thus, the method can be used for early diagnosis of premalignant skin lesions, as well as to evaluate the response to photodynamic treatment.

5. References

[1] Silveira FL, Pacheco MTT, Bodanese B, Pasqualucci C, Zangaro R, Silveira L, "Discrimination of non-melanoma skin lesions from non-tumor human skin tissues in vivo using Raman spectroscopy and multivariate statistics", Lasers Surg Med **47**, 6–16 (2015).

[2] Vyumvuhore R, Tfayli A, Manfait M, Baillet-Guffroy A., "Vibrational spectroscopy coupled to classical least square analysis a new approach for determination of skin moisturizing agents' mechanisms", Ski Res Technol **4**, 282–292 (2014).

[3] Tosi G, Conti C, Giorgini E, Ferraris P, Garavaglia MG, Sabbatini S, Staibano S, Rubini C., "FTIR microspectroscopy of melanocytic skin lesions: A preliminary study", Analyst **135**, 3213–3219 (2010)

[4] Cassio A. Lima, Viviane P. Goulart, Luciana Correa, Thiago M. Pereira, Denise M. Zezell, "ATR-FTIR Spectroscopy for the assessment of biochemical changes in skin due to cutaneous squamous cell carcinoma", Int J Mol Sci **16**, 6621–6630 (2015).

[5] Cassio A. Lima, Viviane P. Goulart, Luciana Correa, Denise M. Zezell, "Using Fourier Infrared spectroscopy to evaluate biological effects induced by photodynamic therapy", Lasers Surg Med, *available online* (2016).

[6] E. Abel, J. Angel Angel J, Kiguchi K, DiGiovanni J. "Multi-stage chemical carcinogenesis in mouse skin: Fundamentals and applications", Nat Protoc **9**, 1350–1362 (2009).

[7] Z. Movasaghi, S. Rehman, IU. Rehman, "Fourier transform infrared (FTIR) spectroscopy of biological tissues", Appl Spectrosc Rev **43**, 134–179 (2008).

Acknowledgments

This work was supported by FAPESP CEPID 05/51689-2, CAPES PROCAD 88881.068505/2014-01; CNPq INCT 573.916/2008-0 and PQ 312397/2013-5.